Coupled Dynamic Analysis of Thruster-Assisted Turret-Moored FPSO

Sangsoo Ryu and M. H. Kim, Texas A&M University

Coastal and Ocean Engineering Division
Dept. of Civil Engineering, Texas A&M University
College Station, Texas 77843, USA.
sryu@tamu.edu, m-kim3@tamu.edu

***Abstract*-To reduce large motion responses of a turret-moored Floating, Production, Storage and Offloading (FPSO) unit in harsh environment in deep waters, a thruster-assisted position mooring (POSMOOR) system can be applied. By applying the system, global dynamic responses can be improved in terms of the mooring line/riser top tensions, operational radius of the FPSO, and the top and bottom angle of the production risers. Kalman filtering as an optimum observer and estimator for stochastic disturbances is implemented in the developed control algorithm to filter out wave frequency components. Investigation of the performance of a thruster-assisted turret-moored FPSO was conducted in terms of surge, sway, yaw motions, and tension time series by using a fully coupled hull/mooring/riser dynamic analysis program in time domain. The two cases, motion analysis of an FPSO with thrusters and without thrusters, are extensively compared. The numerical examples illustrate that a thruster-assisted turret-moored FPSO can be an effective solution compared to a conventional turret-moored FPSO for deepwater production.**

I. INTRODUCTION

As the current major oil and gas fields in the Gulf of Mexico (GoM) are getting depleted, new potential fields in ultra-deep seas (i.e., greater than 2,000m water depth) are getting more and more attention. Applicable deepwater system types consist of compliant towers (CTs), conventional tension leg platforms (TLPs), mini-TLPs, semi-FPSs (floating production systems), truss spars, classic spars, control buoys (CBs) and floating production storage and offloadings (FPSOs). FPSOs are among the most promising offshore structures in ultra-deep seas because they have large storage capacity compared to others and thus overcome the lack of pipeline infrastructure. In addition, they can be used for testing and early production, and the disconnectable turret-riser systems allow FPSOs to sail away from the operational locations for safety purposes when FPSOs face harsh environmental conditions. One example of how to seek a deep water solution is shown in Fig. 1.

Two types of positioning systems were suggested in [1]: dynamic positioning (DP) systems used for positioning of freely floating offshore structures and thruster-assisted position mooring (POSMOOR) systems used for moored structures.

Mooring line systems have been used to keep structures in position. For the station-keeping FPSOs although conventional wire and chain moorings can be applied, the costs of moorings must increase significantly with water depth. On the other hand, a DP system or thruster-assisted POSMOOR performs well both in deep and shallow water and the costs do not increase significantly as moorings [2].

A comprehensive large-scale model test and numerical simulations were conducted [3], and the results emphasize that the full DP FPSO system is a feasible and cost-efficient solution for the ultra-deep water oil/gas development. However, a thruster-assisted turret-moored FPSO may be a more popular solution in deep waters because the offshore platforms should endure harsh environmental conditions and operate for relatively longer period of time as opposed to other full DP applications, such as pipelaying, drilling, diving support, submarine salvage, etc., used in relatively short term offshore operations.

Therefore, the thruster-assisted POSMOOR system is a reasonable solution, and it is already used to maintain the position of turret-moored FPSOs in deep seas [4]. Thruster-assisted turret-moored FPSOs are expected to actively operate in the GoM in the near future as many of them are in operation in the North Sea and have been studied for the GoM [3,5]. Currently, a JIP has already demonstrated the feasibility of maintaining a large FPSO on position in extreme conditions in the GoM using a DP thruster system [3].

Cost-effectiveness is very crucial for a production system in ultra-deep water. Since no wave basin can correctly scale the entire ultra-deep water system, reliable numerical tools will play a very important role. Another important issue concerning the global analysis of offshore structures in deep waters is what analysis does give most reliable answers. It has been studied that uncoupled

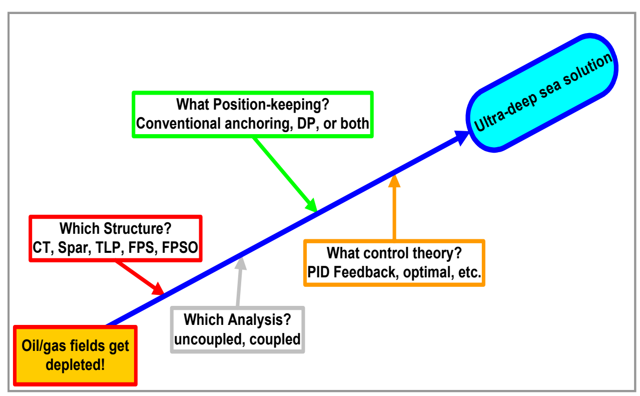

Fig. 1. Diagram that explains one example to seek a possible deepwater solution.

analysis might give inaccurate results especially for deep-water problems [6]. In ultra-deep seas, the mass and length of mooring lines and risers become greater and thus accurate estimate of the damping and inertia effects of mooring lines and risers on the hull motions can only be achieved by the fully coupled analysis program.

However, a coupled motion analysis for a thruster-assisted FPSO has not been studied. This paper will focus on a new approach which is a coupled dynamic analysis of a thruster-assisted turret-moored FPSO and address a conceptual study through relevant numerical simulations of the FPSO in hypothetically deep water on the basis of an assumption that common thruster specification is not given.

II. LITERATURE REVIEW

For deepwater floating structures, vessel motions would be more influenced by moorings and risers. Therefore, water depth becomes deeper, the uncoupled quasi-static analysis, which assumes that moorings/tendons and risers respond statically to the motion of the structure, may produce inaccurate results [6,7]. In this regard, the hull/mooring/riser coupled analysis of a tanker based turret-moored FPSO designed for 1,829m (6,000ft) water depth was carried out in [8] using a coupled dynamic analysis tool called WINPOST-FPSO. On the other hand, Lee, Ha, and Kim [9] considered control performance of a turret-moored vessel assisted by DP system by developing a nonlinear simulator and designing a robust two-degree of freedom controller. They conducted numerical simulations of the nonlinear responses of the FPSO for both the station-keeping mode and tracking mode and concluded that the control system worked satisfactorily. However, in the paper restoring forces of mooring lines were estimated by the catenary equation and regarded as quasi-static.

To design full DP or thruster-assisted POSMOOR systems, a three-degree of freedom problem is generally adequate for the dynamic analysis [10]. However, Sorensen and Strand [11] discussed coupling effects between the horizontal plane (surge, sway, and yaw) and the vertical plane (heave, roll and pitch). They stressed that undesirably large roll and pitch oscillations may be induced by the thruster actions for certain marine structures such as semi-submersibles since they have small water-plane area and low metacentric height, resulting in relatively low hydrostatic coupling phenomena between the vertical plane and the horizontal plane. It was also pointed out that the natural periods of roll and pitch motions typically in the range of 35-65 seconds are within the bandwidth of the positioning controller. They proposed a new multivariable control law to account for motion coupling between the two planes.

A nonlinear passivity-based state observer was developed for a thruster-assisted turret-moored FPSO, and the reduction of the number of tuning parameters was addressed [1]. However, a quasi-static approach was used for a mooring system in this study.

III. FRAMEWORK FOR VESSEL POSITIONING

This paper will deal with a possible oil industry deep water solution, thruster-assisted turret-moored FPSO, by emphasizing on the change of the structural behavior affected by the thruster-assisted POSMOOR system.

The key elements in a vessel positioning system consist of wave filtering, controller design, hydrodynamic motion analysis, and thrust allocation.

A. Reference Frames

Two different reference frames are used: Earth-fixed frame (X, Y, Z) and body-fixed frame (x, y, z). The center of turret is set as the origin of the body-fixed frame. (See Fig. 2.)

B. Continuous-time Kalman Filter for Wave Filtering

The computation of optimal estimates of the states should be a key part of the design processes of an offshore vessel control system. A Kalman filter is most commonly used for a vessel positioning system, tracking, detection, etc. Its filtering algorithm and functionality is adequate to filter out wave frequency (WF) signal in such complicated stochastic problems as measurement and noise reduction in offshore engineering in real-time application. Digital filters can also be used but they may have a time shift problem depending on resolution, filter order, and cutoff frequency, when a real-time application is needed [9].

In this study a Kalman filter is used for optimal estimation of FPSO responses and for the removal of the external forces which include both the leg (i.e. mooring line or riser) forces and the WF components of the environmental forces. A detailed study on a DP system based on Kalman filtering and optimal control was conducted and can be found in [12]. The advantage of a self-tuning Kalman filter over extended Kalman filtering DP systems is also addressed in [13].

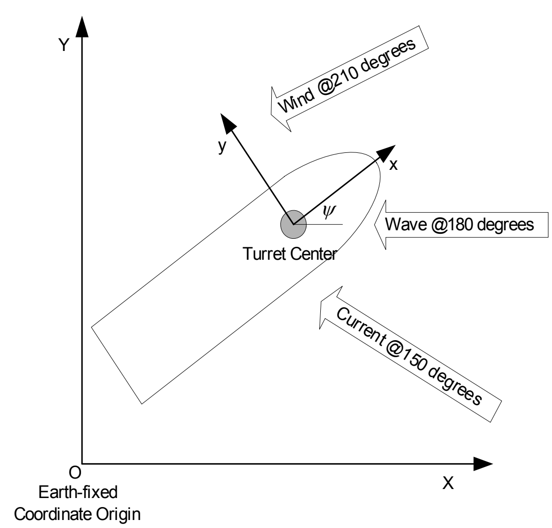

Fig. 2. Schematic diagram of coordinate convention and example of environmental forces.

To design an observer, consider the low frequency (LF) ship model which is linear, time-invariant system of the form [9,10],

$$\dot{\mathbf{x}} = \mathbf{A}\mathbf{x} + \mathbf{B}\mathbf{u} + \mathbf{E}\mathbf{w} \tag{3.1}$$

$$\dot{\mathbf{y}} = \mathbf{C}\mathbf{x} + \mathbf{v} \tag{3.2}$$

where dot $(\cdot)$ denotes time derivative and the each vector written in lower cases can be described by the following set of definitions:

State	$\mathbf{x} = [u, x, v, y, \omega, \psi]^T$
Control Input	$\mathbf{u} = [\tau_x, \tau_y, \tau_\psi]^T$
Plant Noise	$\mathbf{w} = [w_x, w_y, w_\psi]^T$
Measurement	$\mathbf{y} = [x, y, \psi]^T$
Measurement Noise	$\mathbf{v} = [v_x, v_y, v_\psi]^T$.

And the each matrix in (3.1) and (3.2) can also be expressed as follows:

$$\mathbf{A} = \mathbf{M}^{-1}\begin{bmatrix} 0 & 0 & 0 & 0 & 0 & 0 \\ 1 & 0 & 0 & 0 & 0 & 0 \\ 0 & 0 & 0 & 0 & 0 & 0 \\ 0 & 0 & 1 & 0 & 0 & 0 \\ 0 & 0 & 0 & 0 & 0 & 0 \\ 0 & 0 & 0 & 0 & 1 & 0 \end{bmatrix}$$

$$\mathbf{B} = \mathbf{G} = \mathbf{M}^{-1}\begin{bmatrix} 1 & 0 & 0 \\ 0 & 0 & 0 \\ 0 & 1 & 0 \\ 0 & 0 & 0 \\ 0 & 0 & 1 \\ 0 & 0 & 0 \end{bmatrix}$$

$$\mathbf{C} = \begin{bmatrix} 0 & 1 & 0 & 0 & 0 & 0 \\ 0 & 0 & 0 & 1 & 0 & 0 \\ 0 & 0 & 0 & 0 & 0 & 1 \end{bmatrix}$$

$$\mathbf{M} = \begin{bmatrix} M_{11} & 0 & 0 & 0 & 0 & 0 \\ 0 & 1 & 0 & 0 & 0 & 0 \\ 0 & 0 & M_{22} & 0 & M_{26} & 0 \\ 0 & 0 & 0 & 1 & 0 & 0 \\ 0 & 0 & M_{62} & 0 & M_{66} & 0 \\ 0 & 0 & 0 & 0 & 0 & 1 \end{bmatrix}$$

where $M_{11} = m + a_{11}(0)$

$M_{22} = m + a_{22}(0)$

$M_{26} = m + a_{26}(0)$

$M_{62} = m + a_{62}(0)$

$M_{66} = I + a_{66}(0)$

and m the mass of the vessel, I the inertia moment in z-direction, and $a_{ij}(0)$ added masses in LF. Now, let the LF estimated state vector $\hat{\mathbf{x}}$,

$$\hat{\mathbf{x}} = [\hat{u}, \hat{x}, \hat{v}, \hat{y}, \hat{\omega}, \hat{\psi}]^T . \tag{3.3}$$

In (3.1) and (3.2) two noise vectors $\mathbf{w}$ and $\mathbf{v}$ are assumed as vectors of mutually uncorrelated zero-mean Gaussian white noise signals describing the WF external disturbance forces, including first-order wave exciting force, and WF responses, respectively. And their covariance matrices are:

$$\mathbf{Q} = E\left[\mathbf{w} \cdot \mathbf{w}^T\right], \quad \mathbf{R} = E\left[\mathbf{v} \cdot \mathbf{v}^T\right] \tag{3.4}$$

where E represents the time average. Finally, the estimator is therefore proposed in the structure

$$\dot{\hat{\mathbf{x}}}(t) = \mathbf{A}\hat{\mathbf{x}}(t) + \mathbf{B}\mathbf{u}(t) + \mathbf{L}(t)\left[\mathbf{y}(t) - \mathbf{C}\hat{\mathbf{x}}(t)\right] \tag{3.5}$$

where $\mathbf{L}(t)$ is the continuous-time Kalman gain, and it is given by

$$\mathbf{L}(t) = \mathbf{P}\mathbf{C}^T\mathbf{R}^{-1} \tag{3.6}$$

where $\mathbf{P}$ is the solution of the following differential matrix Riccati equation, independent of the gain $\mathbf{L}$.

$$\mathbf{0} = \dot{\mathbf{P}} = \mathbf{A}\mathbf{P} + \mathbf{P}\mathbf{A}^T - \mathbf{P}\mathbf{C}^T\mathbf{R}^{-1}\mathbf{C}\mathbf{P} + \mathbf{G}\mathbf{Q}\mathbf{G}^T \tag{3.7}$$

C. Control Algorithm

Consideration of the excessive thruster modulation gives us the common fact that it is not desirable to counteract the WF motion caused by first-order wave exciting forces. Only slowly varying signals which are originated mainly from second-order mean and slowly varying environmental forces need to be obtained through a filter and those filtered signals are used for control algorithm. In this study a PID (Proportional-Integral-Derivative) controller is adopted, and the integral gains D_I and P_I are set to zero by assuming that the error integral is not significant. However, in general steady-state errors due to wind, current and wave drift can all be compensated for by adding integral action to the control law.

The required control input vector $\mathbf{u}$ (thrust) is calculated based on the following PD control theory,

$$\mathbf{u} = -\mathbf{K}(\hat{\mathbf{x}} - \mathbf{x}_{set}) \tag{3.8}$$

where the PD gain matrix $\mathbf{K}$ is:

$$\mathbf{K} = \begin{bmatrix} D_x & P_x & 0 & 0 & 0 & 0 \\ 0 & 0 & D_y & P_y & 0 & 0 \\ 0 & 0 & 0 & 0 & D_\psi & P_\psi \end{bmatrix} \tag{3.9}$$

where D and P denote derivative and proportional gains, respectively. An overall concept of this vessel control system can be summarized in Fig. 3 [14].

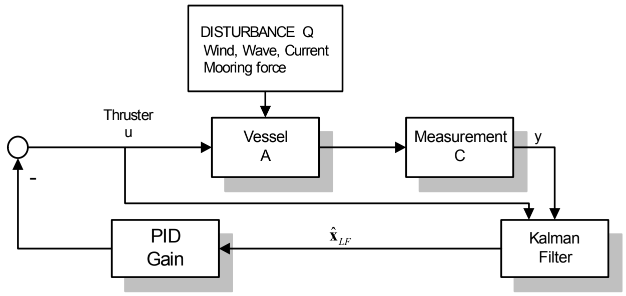

Fig. 3. Block diagram of vessel control system.

D. *Thrust Allocation Algorithm*

The calculation of the required thrust $\mathbf{u}$ in (3.8) is followed by a thrust allocation algorithm, which is basically distribution of the thrust to each installed thruster depending on the type (i.e. azimuth, channel, fixed, etc.), power limit, thrust characteristics, and the locations of the thrusters. However, the thrust allocation algorithm was not implemented in this study.

E. *Coupled Analysis*

As water depth increases, the mass of the mooring lines and risers, called "legs," becomes larger and the effect of the dynamic interaction between the vessel and the legs should be considered for a better analysis [15]. It is addressed that the time domain coupled analysis is the most adequate for such cases because mooring lines and risers can significantly influence the hull responses [16]. The analysis is conducted using WINPOST-FPSO, a fully coupled dynamic analysis program developed by Texas A&M University [7]. The computer program considers the mooring line and riser dynamic responses along with the entire range of FPSO responses, including the wave frequency responses, thus the system equations are solved simultaneously in the time domain.

IV. CASE STUDY

A turret-moored FPSO is used for the analysis of the thruster-assisted POSMOOR system described in this paper. The tanker-based FPSO using 12 chain-polyester-chain taut mooring lines with 13 steel catenary risers designed for 1,829m water depth is numerically simulated to investigate the characteristics of nonlinear behaviors and hull/mooring/riser dynamic coupling [15]. The first-order wave-frequency and second-order difference-frequency wave loads, fluid added mass and radiation damping for the hull are calculated in the frequency domain from the second-order diffraction/radiation program WAMIT. The wave-current induced forces on slender members are calculated from Morison formula. The 100-Year Hurricane with non-parallel wind, wave, and current is used as environmental condition. The wind and current forces are calculated from the empirical data provided by OCIMF (Oil Company International Marine Forum) [17].

TABLE 1
MAIN PARAMETERS OF TURRET-MOORED FPSO

Designation	Symbol	Unit	Quantity
Production level		*bpd*	120000
Storage		*bbls*	1440000
Vessel size		*kDWT*	200
Length b/w perpendiculars	Lpp	*m*	310
Breadth	B	*m*	47.2
Depth	H	*m*	28.0
Draft	T	*m*	18.9
Length to beam ratio	L/B		6.57
Beam to draft ratio	B/T		2.5
Displacement	Δ	*ton*	240869
Block coefficient	Cb		0.85
Center of buoyancy Forward section 10	FB	*m*	6.6
Water plane area	A	m^2	13400
Water plane coefficient	Cw		0.9164
Center of water plane area forward section 10	FA	*m*	1.0
Center of gravity above base	KG	*m*	13.3
Metercentric height transverse	MGt	*m*	5.8
Metercentric height longitudinal	MGl	*m*	403.8
Trans. radius of gyration in air	Kxx	*m*	14.8
Long. radius of gyration in air	Kyy	*m*	77.5
Yaw radius of gyration	Kzz	*m*	79.3
Wind area front	Af	m^2	1012
Wind area side	Ab	m^2	3772
Turret in centerline Behind Fpp (20.5% Lpp)		*m*	63.5
Turret elev. below tanker base		*m*	1.5
Turret diameter		*m*	15.8

A. *Main Parameters of Turret-Moored FPSO*

The prototype FPSO used in this study is a 200,000 DWT tanker moored in 1,829m water depth by a taut chain-polyester-chain mooring system with a turret. The internal turret is located 63.55m away from the forward perpendicular and its diameter is 15.8m. The main parameters of the turret-moored FPSO are given in Table 1.

The FPSO has a length between perpendiculars of 310m, a width of 47.2m, a depth of 28.0m with a full loaded draft of 18.9m. When OCIMF data were used for wind and current loading, cylindrical bow with full loading condition was selected.

B. *Particulars of Mooring Lines and Risers*

The particulars of the mooring lines and risers are given in Tables 2 and 3. The FPSO has 12 chain-polyester-chain mooring lines and 13 steel catenary risers. The polyester lines may have a range of stiffness under different loading conditions but they are assumed to be elastic in this study with a representative Young's modulus. The 12 mooring lines are arranged in four groups. Each group is 90-degree apart and consists of 3 legs 5-degree apart. (See Fig. 4.) In the dynamic analysis of slender members, tangential drag forces are neglected. The seafloor is modeled as elastic bed with quadratic spring.

The particulars of hull, mooring lines, and risers are almost identical to those of the standard case set up by

DEEPSTAR Offshore Industry Consortium [18] except the two cases. The first one is the angle of mooring lines at the fairlead; here 43 degrees were used instead of 48.8 degrees. The second difference is the angle of riser top connection; 77 degrees were used here instead of 80.9 degrees.

TABLE 2
PARTICULARS OF MOORING LINES

Designation	Unit	Quantity
Water depth	*m*	1829
Pre-tension	*kN*	1424
Number of lines		4×3
Degree between the 3 lines	*deg.*	5
Length of mooring line	*m*	2652
Radius of location of chain stoppers on turn table	*m*	7.0
SEGMENT 1(GROUND SECTION): CHAIN		
Length at anchor point	*m*	121.9
Diameter	*cm*	9.52
Dry weight	*N/m*	1856
Weight in water	*N/m*	1615
Stiffness AE	*kN*	912120
Mean breaking load (MBL)	*kN*	7553
SEGMENT 2: WIRE (POLYESTER)		
Length	*m*	2438
Diameter	*cm*	16.0
Dry weight	*N/m*	168.7
Weight in water	*N/m*	44.1
Stiffness AE	*kN*	186800
Mean breaking load (MBL)	*kN*	7429
SEGMENT 1(GROUND SECTION): CHAIN		
Length at anchor point	*m*	91.4
Diameter	*cm*	9.53
Dry weight	*N/m*	1856
Weight in water	*N/m*	1615
Stiffness AE	*kN*	912120
Mean breaking load (MBL)	*kN*	7553

TABLE 3
PARTICULARS OF RISERS

Riser Type	Top Tension	OD	AE	EI	Weight Dry/Wet	Cdn
	kN	cm	kN	kNm^2	N/m	
Liquid Production	2224	44.5	1.83×10^7	276	1927 1036	1
Gas Production	1223	38.6	1.08×10^7	113	1708 525	1
Water Injection	4048	53.1	1.86×10^7	224	2802 1897	1.414
Gas Injection	2714	28.7	3.14×10^6	64	1810 1168	1.414
Gas Export	912	34.3	8.63×10^6	71	1357 423	1
Total Length of Risers			3657.4 m			

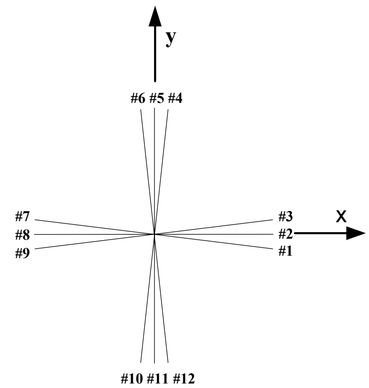

Fig. 4. Arrangement of the FPSO mooring lines.

C. *Numerical Modeling of FPSO Hull*

The added mass and radiation damping, first-order wave-frequency forces, and second-order mean and difference-frequency forces are calculated from the second-order diffraction/radiation program WAMIT [19,20]. Fig. 5 shows the distribution of panels on the body surface. Taking advantage of symmetry, only half domain is discretized (1684 panels for hull and 480 panels for free surface). All the hydrodynamic coefficients were calculated in the frequency domain, and then the corresponding forces were converted to the time domain using two-term Volterra series expansion [21]. The frequency-dependent radiation damping was included in the form of convolution integral in the time domain equation. The wave drift damping was expected to be small and thus not included in the ensuing analysis.

The methodology for hull/mooring/riser coupled statics/dynamics is similar to that of [22,23]. The mooring lines are assumed hinged at the turret and anchor position. The near-vertical riser is also hinged at the turret, and therefore, the riser tension is included in the vertical static equilibrium of the hull. The calculated platform mass for the given condition is 2.3686×10^8 kg at 18.9m draft. The empirical coefficients for the viscous damping of the same FPSO hull in normal direction were obtained from the model test by Wichers [24].

The wave force quadratic transfer functions are computed for 9 wave frequencies, ranging from 0.24 to 1.8

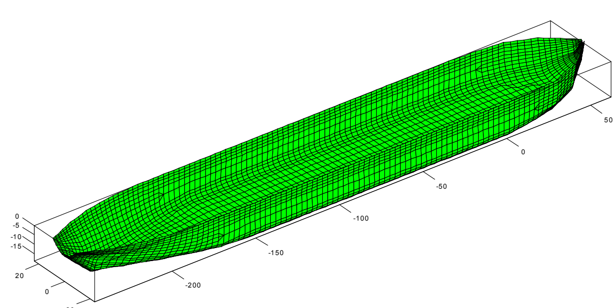

Fig. 5. Mesh generation of the turret-moored FPSO.

rad/sec and the intermediate values for other frequencies are interpolated.

The hydrodynamic coefficients and wave forces are expected to vary appreciably with large yaw angles and the effects should be taken into consideration for the reliable prediction of FPSO global motions. Therefore, they are calculated in advance for various yaw angles with 5-degree interval and the data are then tabulated as inputs.

The second-order diffraction/radiation computation for a 3D body is computationally very intensive especially when it has to be run for various yaw angles. Therefore, many researchers avoided such a complex procedure and have instead used simpler approach called Newman's approximation i.e. the off-diagonal components of the second-order difference-frequency QTFs are approximated by their diagonal values (mean drift forces and moments). The approximation can be justified only when the relevant natural frequency is very small and the slope of QTFs near the diagonal is not large. In this paper, the Newman's approximation is used.

The wind and current force coefficients on the vessel are read from the OCIMF data. The dynamic wind loading was generated from the wind velocities obtained from API wind spectrum. The yaw wind moments are increased by 15% considering the effects of superstructures.

D. Time-Domain Simulation

Note that the derivative and proportional gains, D_ψ and P_ψ in (3.9), are set to zero in this study in order to implement the "automatic weathervaning" feature of a turret by which the FPSO is headed to an optimized yaw angle minimizing environmental forces. By this reason, the feedback heading angle control of the FPSO was not included in this simulation.

The waves are assumed to be uni-directional. A JONSWAP spectrum of significant wave height H_s =12.19m, peak period T_p =14s, and overshoot parameter γ =2.5 was selected to represent a typical 100-yr storm in the GoM. While 10-year storm condition is suggested for full DP system, 100-year hurricane condition is applied in this study. As mentioned in [14], the design sea conditions for a thruster assisted POSMOOR system can be stronger than those considered for a full DP system.

The storm induced current flows from 30-deg. right of wave direction and is assumed to be steady. The current velocity is assumed to be 1.07m/s between 0-61m and reduced to 9.1cm/s at 91m-910m. The wind speed used is 148km/h@10m and its direction is 30-deg. left of waves. The directions of these environmental forces are shown in Fig. 2. API wind spectrum is used for the generation of time-varying wind forces. The drag coefficients for wave forces are 1.0 for mooring lines, 1.0 to 1.414 for risers. The low- and wave-frequency regions are defined as 0-0.2 rad/s and 0.2-1.3 rad/s, respectively. The time-domain simulation results are summarized in Tables 4 and 5.

From Table 4, it is found that slowly varying components of hull responses are reduced when thrusters are applied, and they are dominant in horizontal-plane motions (surge, sway, and yaw), while wave-frequency responses are more important in vertical-plane motions (heave, roll, pitch). The motion amplitude in X-direction is mainly reduced compared to the one in Y-direction (Figs. 6 and 7) because the FPSO is affected by three types of environmental forces arranged closely in X-direction shown in Fig. 2. It can also be noticed that the roll motion responses are increased after applying the thruster forces, which may be influenced by the installation depth the thrusters.

In Table 5, the mean top tension of mooring line No. 2 (taut side) is decreased after applying the thrusters while that of mooring line No. 8 (slack side) is increased. This is because of the direction of the environmental forces and that the taut side becomes less taut and the slack side less slack. At any rate the maximum tension of mooring line 2 is reduced by 25% by applying the position control system. This improvement can be even larger in 10-yr storm environment. As shown in Table 4 and Fig. 6, the overall horizontal-plane motion response is reduced. Therefore, the vessel is closer to the origin and the two mooring line top tensions become closer to those at the undisturbed condition.

TABLE 4
Comparison of Statistical Results
of FPSO Hull Motions (unit: meter, degree)

	Thruster	Mean	LF *rms*	WF *rms*	Total *rms*	Max
Surge	Yes	-6.7	5.03	0.54	5.1	-23.9
	No	-13.9	6.98	0.49	7.0	-34.6
Sway	Yes	3.1	1.95	0.50	2.0	9.8
	No	4.7	2.50	0.49	2.5	13.4
Heave	Yes	0.1	0.04	0.81	0.8	2.9
	No	0.0	0.04	3.36	3.4	10.9
Roll	Yes	0.1	0.19	1.93	1.9	5.7
	No	0.2	0.16	0.98	1.0	3.5
Pitch	Yes	0.0	0.05	0.82	0.8	2.9
	No	0.0	0.02	1.33	1.3	-4.3
Yaw	Yes	17.2	2.12	0.30	2.1	23.3
	No	15.3	2.74	0.28	2.6	22.7

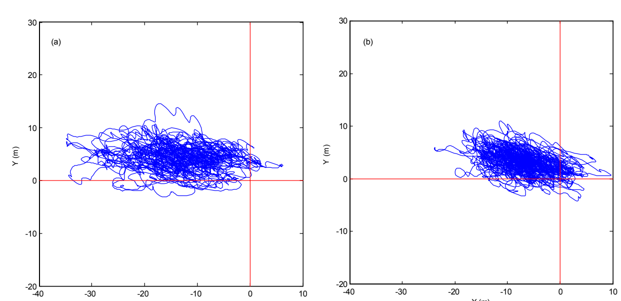

Fig. 6. Comparison of the turret position trajectories simulated (a) without thruster-assisted system and (b) with one. The total time duration is 150 minutes.

TABLE 5
COMPARISON OF MOORING LINE/RISER TOP TENSIONS (UNIT: KN)

Leg Type and ID #	Thruster	Mean	Total *rms*	Max
Mooring Line #2	Yes	1773	263	2743
	No	2201	479	3639
Mooring Line #8	Yes	1134	218	1928
	No	901	296	2077
Liquid Production Riser #13	Yes	2323	107	2714
	No	2343	262	5393
Gas Production Riser #20	Yes	1239	116	1622
	No	1254	265	3213
Water Injection Riser #22	Yes	4249	157	4793
	No	4383	391	6923
Gas Injection Riser #23	Yes	2728	100	3049
	No	2746	227	4054
Gas Export Riser #25	Yes	949	75	1197
	No	961	166	1781

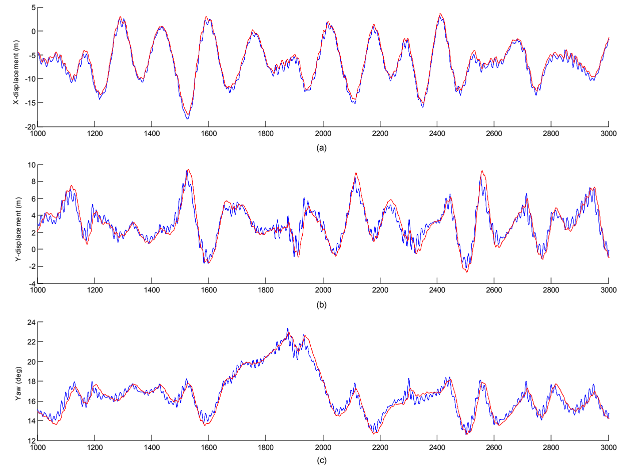

Fig. 8. Displacement time series of original signals (blue) and their low frequency estimates (red) at the turret center obtained by applying Kalman filter: (a) X-disp, (b) Y-disp, and (c) yaw.

The simulation results of riser top tensions are quite different from those of mooring lines. The mean of the top tension does change slightly but the total *rms* values obtained with thruster-assisted system are reduced by more than 50%. By this reason, the maximum tensions are also reduced. This clearly demonstrates the benefit of employing thruster-assisted positioning system.

To check the Kalman filter, the estimates of hull displacement and velocity were observed and shown in Figs. 8 and 9. Translational velocity in Y-direction and rotational velocity in Z-direction show correctly filtered signals and slight up-shift is found in the velocity in X-direction. The reason may be the absence of the damping term in the Kalman filter design of the LF equation of motion (3.1) and of an optimal control routine to calculate PID gains. In turret-moored FPSO simulations, three horizontal-plane motion responses are already LF motions, but velocities are high frequency variables which need wave filtering.

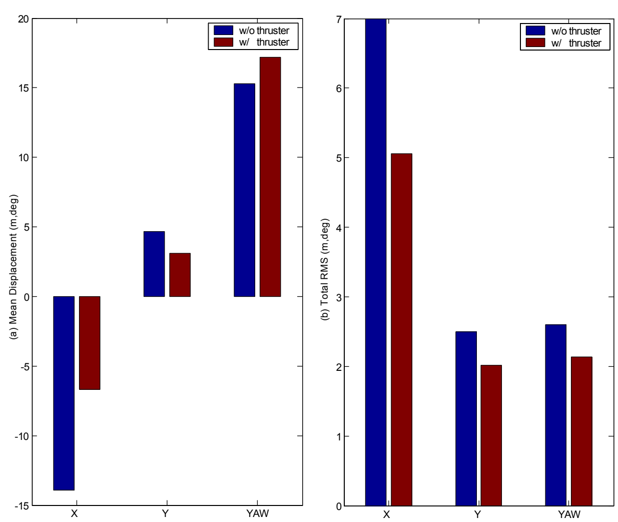

Fig. 7. Statistical analysis of the horizontal-plane motion of the turret center. Comparisons of (a) mean displacement and (b) total *rms* of two cases: no thruster force and with thruster forces.

V. CONCLUSIONS AND FUTURE WORK

In this paper, a fully coupled dynamic analysis of a thruster-assisted turret-moored FPSO was conducted. It is clearly demonstrated that the vessel horizontal-plane responses as well as mooring and riser tensions can be significantly reduced by applying the thruster-assisted positioning system. The riser mean top tensions remain almost the same, while the *rms* values are significantly reduced to make extreme values appreciably smaller.

To implement the weathervaning, PD gains for yaw angle were set to zero. Statistical analysis for the yaw motion shows that mean yaw angle was affected by the direction of wind forces, and the mean position of the center of turret was mainly affected by current force in this case study. Of course, the weathervaning feature in turret-moored FPSOs would find the optimum yaw angle

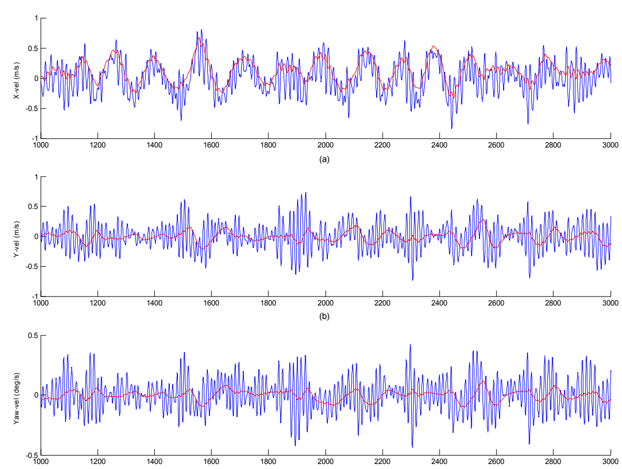

Fig. 9. Velocity time series of original signals (blue) and their low frequency estimates (red) at the turret center obtained by applying Kalman filter: (a) X-vel, (b) Y-vel, and (c) yaw-vel.

minimizing environmental forces without the help of the thruster-assisted positioning system.

This paper stresses that thruster-assisted turret-moored FPSOs can be a possible cost-effective and safety-concerned solution for the ultra-deep water development. The fully coupled hull/mooring/riser dynamic program in time domain can be used to assess the overall performance and enhancement of the system after applying a thruster-assisted positioning system. In this regard, the fully coupled dynamic analysis program WINPOST-FPSO-DP was developed. And the numerical results show that assisting thrusters can significantly increase the global performance of the FPSO hull motions and reduce the tension stresses of the mooring lines and risers.

Thrust allocation algorithm, thruster power specification, implementation of the integral action, wind feedforward, autotuning of PID gains based on optimal control theory need to be considered in the further study.

Acknowledgments

Authors are grateful for the financial support by the Offshore Technology Research Center and the Minerals Management Service.

References

[1] A.J. Sorensen, J.P. Strand, and T.I. Fossen, "Thruster assisted position mooring system for turret-anchored FPSOs," *Proc. of the IEEE Conference on Control Applications*, Hawaii, US.

[2] N.D.P. Barltrop, "Floating Structures: a guide for design and analysis," Center for Marine and Petroleum Technology, Vol.2, 1998.

[3] J.L. Cortijo, A.S. Duggal, R. Dijk, and S. Matos, "DP FPSO – A fully dynamically positioned FPSO for ultra deep waters," *Proc. of ISOPE 2003*, Honolulu, Hawaii, USA, May 25-30, pp. 194-202.

[4] D.H. Lee and H.S. Choi, "A dynamic analysis of FPSO-Shuttle Tanker System," *Proc. 10th Int. Offshore and Polar Eng. Conference*, Seattle, USA, 2000.

[5] J. Wichers and R. Dijk, "Benefits of using assisted DP for deepwater mooring systems," *Offshore Technology Conference*, OTC 10781, Houston, USA, 1999.

[6] W. Ma, M.Y. Lee, J. Zou, and E. Huang, "Deepwater nonlinear coupled analysis tool," *Proc. of Offshore Technology Conference*, OTC 12085 [CD-ROM], Houston, Texas, 2000.

[7] T. Arcandra, "Hull/mooring/riser coupled dynamic analysis of a deepwater floating platform with polyester lines," Ph.D. Dissertation, Texas A&M University, 2001.

[8] T. Arcandra, P. Nurtjahyo, and M.H. Kim, "Hull/mooring/riser coupled analysis of a turret-moored FPSO 6000ft: Comparison between polyester and buoys-steel mooring lines," *The 11th Offshore Symposium*, The Texas Sec. of SNAME, Houston, Texas, 2001.

[9] D.Y. Lee, M.K. Ha, and H.J. Kim, "Development of dynamic positioning simulation program," *J. Kansai Soc. N. A.*, Japan, No. 231, March 1999, pp. 65-73.

[10] T.I. Fossen, *Guidance and Control of Ocean Vehicles*, John Wiley & Sons Ltd., 1994.

[11] A.J. Sorenson and J.P. Strand, "Positioning of semi-submersibles with roll and pitch damping," *Control Applications in Marine Systems*, Int. Federation of Automatic Control, Fukuoka, Japan, 1998.

[12] J. Balchen, N. Jenssen, E. Mathisen, and S. Saelid, "A dynamic positioning system based on Kalman filtering and optimal control," *Modeling, Identification and Control*, 1980, pp. 135-163.

[13] P.T. Fung and M.J. Grimble, "Dynamic ship positioning using a self-tuning Kalman filter," IEEE Trans. on Automatic Control, Vol. AC-28, No. 3, 1983, pp. 339-350.

[14] A.B. Aalbers, S.A.W. Janse, and W.C. Boom, "DP assisted and passive mooring for FPSO's," *Offshore Technology Conference*, OTC 7722, Houston, USA, 1995, pp. 281-288.

[15] Y.B. Kim and M.H. Kim, "Hull/mooring/riser coupled dynamic analysis of a tanker-based turret-moored FPSO in deep water," *Proc. of ISOPE 2002*, Kyushu, Japan.

[16] Y. Luo and S. Baudic, "Predicting FPSO responses using model tests and numerical analysis," *Proc. of ISOPE 2003*, Honolulu, Hawaii, USA, May 25-30, pp. 167-174.

[17] OCIMF, *Prediction of wind and current loads on VLCCs*, 2nd ed., Witherby & Co. Ltd., London, England, 1994.

[18] J.E.W. Wicher and P.V. Devlin, "Effect of coupling of mooring lines and risers on the design values for a turret moored FPSO in deep water of Gulf of Mexico," *Proc. of 11th Intl. Offshore & Polar Engr.*,Vol.3, 2001, pp. 480-487.

[19] F.T. Korsmeyer, C.H. Lee, J.N. Newman, and P.D. Sclavounos, "The analysis of wave effects on TLP," *Proc. of OMAE'88*, Houston, 1988.

[20] C.H. Lee, J.N. Newman, M.H. Kim, and D.K.P Yue, "The computation of second-order wave loads," *Proc. of OMAE'91*, Stavanger, Norway, 1991.

[21] Z. Ran, M.H. Kim, J.M. Niedzwecki, and R.P. Johnson, "Responses of a spar platform in random waves and currents (experiment vs. theory)," Proc. of ISOPE'95, Hague, Netherlands, 1995.

[22] Z. Ran and M.H. Kim, "Nonlinear coupled analysis of a tethered spar in waves," *J. of Offshore & Polar Engr.* Vol.7, No.2, 1997, pp. 111-118.

[23] M.H. Kim, Z. Ran, and W. Zheng, "Hull/mooring coupled dynamic analysis of a truss spar in time domain," *Proc. of ISOPE'99*, Brest, France, 1999.

[24] J.E.W. Wicher and C. Ji, "On the coupling term in the low-frequency viscous reation forces moored tankers in deep water," *Proc. of Offshore Technology Conference*, OTC 12086 [CD-ROM], Houston, Texas, 2000.